Environ Earth Sci (2015) 73:6663–6676
DOI 10.1007/s12665-014-3888-z

ORIGINAL ARTICLE

Temporal variability of soil organic carbon transport in the Enxoé agricultural watershed

T. B. Ramos · S. Rodrigues · M. A. Branco · A. Prazeres · D. Brito · M. C. Gonçalves · J. C. Martins · M. L. Fernandes · F. P. Pires

Received: 1 April 2014 / Accepted: 15 November 2014 / Published online: 26 November 2014
© Springer-Verlag Berlin Heidelberg 2014

Abstract The temporal variability of particulate (POC) and dissolved (DOC) organic carbon concentrations was analyzed in the Enxoé temporary river, southern Portugal, between September, 2010 and August, 2013. The overall aim was to study the variability of those elements during storm events, and determine their origin and the main transfer mechanisms to the river. Twenty-one flood events were observed. An empirical model was used to describe changes in solute concentrations, and the magnitude and rotational patterns of the hysteretic loops during flood events. POC and DOC concentrations varied between 0.49–88.93 and 0.25–25.75 mg L^{-1}, respectively. POC and DOC annual yields varied between 0.06–2.15 and 0.03–1.47 t km^{-2}, respectively. Flood events had greater effect in POC than in DOC variability. POC had mostly a terrestrial origin, with exports being related to soil erosion and runoff. POC revealed a flushing behavior during the entire monitored period, and clockwise or anticlockwise trajectory loops whenever the predominant origin of the exports was in river bed deposits or arable lands, respectively. DOC had also a terrestrial origin, but it revealed a contrasting dilution behavior and, in general, anticlockwise hysteresis loops. DOC showed a delay in the arrival of solutes to the river, consistent with mass flow through subsurface flow. DOC exports were thus associated with soil weathering and crop mineralization. This work highlights the main processes involved in POC and DOC loads in a temporary river during flood events, with a precise quantification of those elements.

Keywords DOC · Hysteresis · POC · Mediterranean region · Temporary rivers

T. B. Ramos (✉) · D. Brito
MARETEC, Instituto Superior Técnico, University of Lisbon, Av. Rovisco Pais, no 1, 1049-001 Lisboa, Portugal
e-mail: tiago_ramos@netcabo.pt

S. Rodrigues · M. A. Branco · A. Prazeres · M. C. Gonçalves · J. C. Martins · M. L. Fernandes · F. P. Pires
INIAV, Instituto Nacional de Investigação Agrária e Veterinária, Oeiras, Portugal

Introduction

Flood events are recognized as the most effective process for driving sediments and sediment-bound pollutants (pesticides, particulate, nutrients, heavy metals, and other toxic substances) into rivers and lakes on a short time scale, leading to aquatic habitat degradation and to the contamination of drinking water and ecosystems. Many hydrological studies have shown how the river exports vary significantly in magnitude and frequency along the year as a result of those episodic event discharges (Oeurng et al. 2011; Zhu et al. 2012; Cerro et al. 2013). These studies typically require monitoring programs with a high sampling density focusing on the hydrological and biogeochemical regimes of the studied rivers, which are still very rare in the particular case of temporary Mediterranean rivers.

Temporary Mediterranean rivers and streams are generally ungauged due to their restricted economic importance (Tzoraki and Nikolaidis 2007). Sediment and contaminant dynamics in temporary rivers is mainly determined by sequences of dry periods and the following flood events (Lillebø et al. 2007), providing a significant challenge in developing sustainable water management plans. The Enxoé temporary river, located in semi-arid southern Portugal, is a good example where effective conservation measures need to be put into practice. The

river flows to the water reservoir with the highest eutrophic state in Portugal (Instituto da Água 2008), but which supplies close to 25000 inhabitants. Ramos et al. (2014) have recently identified the main origins of the sediments and nutrients (P and N) being flushed to the Enxoé reservoir and their respective transfer mechanisms. We now focus on the dynamics of particulate (POC) and dissolved (DOC) organic carbon forms, which are an important factor in stream water quality and an indicator of organic contamination.

Organic carbon (OC) transport from terrestrial ecosystems to marine systems represents an important process in the global carbon cycling. The dissolved form contributes to the transport of heavy metals and organic micropollutants, acts as an energy source, affects light penetration, plays a role in pH buffering, controls the partition of components between water and sediment, is a source of nutrients, and represents a major issue in the treatment of water (Veum et al. 2009; Worrall et al. 2012; Strohmeier et al. 2013). POC, normally bounded to sediments, further contributes to the loss of water storage capacity in reservoirs, and constitutes an indicator of soil erosion and land degradation (Oeurng et al. 2011; Némery et al. 2013). OC transport is strongly associated with catchment physical characteristics (Hope et al. 1997; Lu et al. 2012; Oh et al. 2013), but the underlying factors that control exports are still only partially understood. Thus, there is a need for studies focusing on OC concentrations and fluxes in temporary rivers, particularly during flood events, to better understand the mechanisms and processes associated and their relations with edafo-climatic conditions and land uses (Butturini et al. 2008; Oeurng et al. 2011; Strohmeier et al. 2013).

Interpreting POC and DOC delivery processes using hysteresis patterns may help to understand the origin of those elements in a catchment and respective transfer mechanisms into rivers (House and Warwick 1998; Oeurng et al. 2011; Strohmeier et al. 2013). Hysteresis, at a given discharge (Q), is characterized by differences in the concentration (C) of an element on the rising and falling limb of a hydrograph (Hall 1970). Recurrent $C-Q$ patterns of a specific solute can then be detected using simple methods which require only a few parameters (Evans and Davies 1998; House and Warwick 1998; Bowes et al. 2005; Butturini et al. 2006). These methods can help identifying solute origin and the transfer mechanisms in detail. However, the analysis of C–Q responses in Mediterranean streams is still in a preliminary phase, and even rarer are those studies that explored these responses in Mediterranean human-altered systems, like Enxoé.

The objectives of this paper are: (i) to present the temporal variability in POC and DOC transport in the Enxoé River (southern Portugal) during three hydrological years (September, 2010 to August, 2013); (ii) to determine POC and DOC loads to the Enxoé reservoir at the outlet of the watershed during the monitored period; and (iii) to identify POC and DOC source areas and processes associated based on the interpretation of hysteresis in the C–Q relationship. The results permit to have data on OC loads during storm events in the case of temporary rivers, and pretend to help decision-makers to improve the management of drinking water catchments areas by minimizing organic contamination risks during flood events.

Materials and methods

Catchment description

The Enxoé catchment is located in the Alentejo region, southern Portugal (Fig. 1). The river is a tributary of the Guadiana River, has a bed length of 9 km, and catchment area of 60.80 km^2. The dominant soils are Luvisols, Cambisols, and Calcisols. The main land uses are olive groves, agro-forestry of holm-oaks, and annual winter crops. The climate in the region is dry sub-humid to semi-arid. The annual average precipitation is 500 mm, with 80 % concentrated between October and April. The annual average temperature is 16 °C, and the annual reference evapotranspiration varies between 1,200 and 1,300 mm. The catchment has a population of 1,000 inhabitants, mainly concentrated in Vale de Vargo, and is limited downstream by a dam (10.4 million m^3). Weather data used in this study were collected from a weather station located in Serpa (Fig. 1).

River Enxoé water quality monitoring

The river Enxoé water was monitored from September, 2010 to August, 2013 at a sampling station located at the outlet of the watershed before the reservoir (Fig. 1). The upstream drainage area covers approximately 45 km^2. Sampling waters was for suspended sediment concentration (SSC), POC, and DOC. An YSI 6920 measuring probe (YSI Incorporated, Ohio, USA) was used to monitor the water stream level and turbidity (nephelometry). Readings were taken every 15 min during flood events and daily during non-flood events. Flow was obtained from the measured water level and the shape of the river bed with the well-established Gauckler–Manning formula. An automatic water sampler (EcoTech Umwelt-Meßsysteme GmbH. Bonn, Germany) with 8 bottles, 2 L each, was used for monitoring water quality during floods. The monitoring station was positioned near the bank of the river, where the homogeneity of water movement was considered representative of all hydrological conditions. The pump inlet of

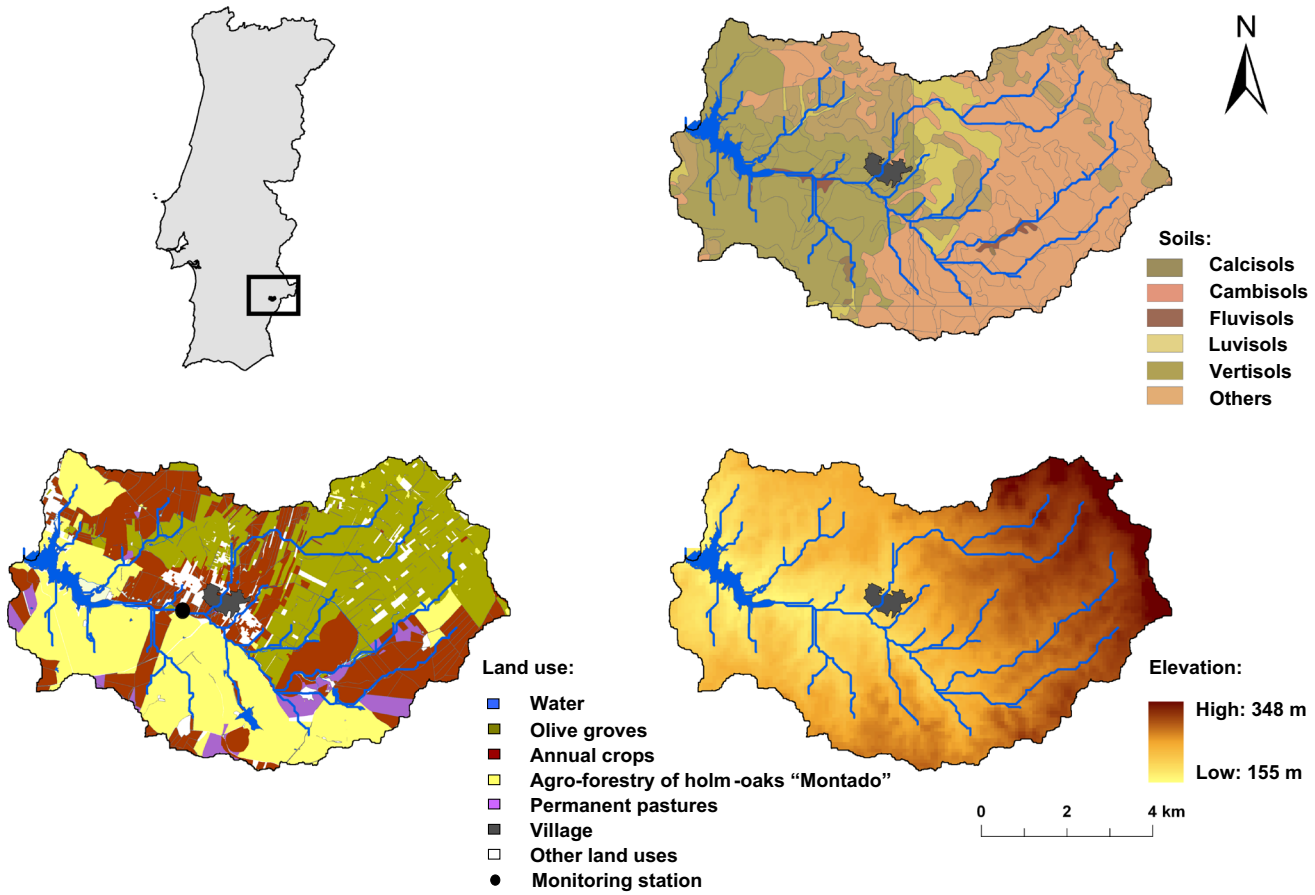

Fig. 1 Location (*top left*), land use (*bottom left*), major soil units (*top right*), and digital elevation model (*bottom right*) in Enxoé catchment area

the automatic water sampler was placed next to the measuring probe pipe. The probe was programmed to activate the automatic water sampler when the water level varied more than 10 cm on both rising and falling stages of flood events (variations of 3 min to 15 h during flood events). Manual sampling was also carried out at weekly intervals using 2 L bottles collected near the probe location. The total number of water samples taken from both automatic and manual sampling was 176.

Water samples (250–1,000 mL) were filtered in the laboratory to determine SSC using pre-weighed glass microfiber paper (GFF 0.75 µm). The sediments retained on the filter paper were oven dried at 50° C during 24 h. The filters were again weighed and SSC was calculated. SS retained in the dried filters were then acidified with HCl 2 N and dried at 60 °C for 24 h to remove the carbonates. POC analysis was carried out in the remaining SS using a LECO CNS2000 analyzer. POC content was expressed as a percentage of dry weight of sediment and converted to POC concentration (M L^{-3}).

The same water samples, after being filtered for determining SSC and POC, were acidified with HCl (12N; pH 2) and kept cold at 4 °C until DOC was analyzed. DOC analysis was performed using a colorimetric method (closed reflux), in which samples were digested with potassium dichromate and sulfuric acid. Readings were taken with a Thermo Scientific UV visible spectrophotometer using two different wavelengths (340 and 590 nm) depending on carbon concentration in the solution (APHA 1998).

POC and DOC loads

Water yield was determined after integrating river discharge over a time period (3–15 min during flood events and daily during non-flood events), as follows:

$$W = \sum_{i} \frac{\left(Q_{(i)} + Q_{(i-1)}\right)}{2} \times \left(t_{(i)} - t_{(i-1)}\right) \quad (1)$$

where W is the accumulated water yield (L^3), and Q_j is the instantaneous river discharge (L^3 T^{-1}) at time i (T).

POC and DOC yields were obtained by averaging concentrations between two adjacent samples and integrating this with discharge. Continuous POC series were thus developed to significantly reduce uncertainty that would

result from interpolation and extrapolation of low-frequency measurements of POC. The continuous data series were based on the SSC-turbidity, SSC–POC, and POC-turbidity relations found in Enxoé, and on the quasi-continuous turbidity recording provided by the automatic probe which complemented the information collected with the automatic water sampler. Further details can be found in Ramos et al. (2014). DOC was estimated from the high frequency of data collection provided by the automatic sampler. POC and DOC loads were thus linear interpolated between two adjacent samples, as follows:

$$M_d = \sum_i \frac{\left(C_{d\,(i)} + C_{d\,(i-1)}\right)}{2} \times W_i \quad (2)$$

where M_d is the solute mass lost in the catchment from diffuse (d) sources (M), and C_j is the instantaneous solute concentration (M L^{-3}) at time i (T). No point source emissions exist in the Enxoé catchment (Ramos et al. 2014).

Relationships between POC, DOC and hydro-climatological variables

The relationships between POC and DOC concentrations and loads, SS concentrations and loads, and hydro-climatological variables were analyzed to determine the factors controlling POC and DOC transport during flood events. Flood events were defined as complete hydrological events with rising and recession limbs. A database was generated for each discharge peak monitored during flood events, containing three groups of variables: (i) antecedent variables characterizing the situation prior to peak flow; (ii) storm event variables (precipitation and discharge); and (iii) variables related to water quality (SS, POC, and DOC).

Antecedent variables included: accumulated precipitation 1, 5, and 10 days before each discharge peak (P1, P5, and P10); the baseflow before the first peak discharge of a flood event (Q_b); and flow in the end of the falling limb of the antecedent peak flow when multiple peaks occurred during a flood event (Q_a) (Table 1).

Storm event variables comprised: total precipitation during flood events (P_e); the peak number when multiple peaks occurred (P_n); flood duration, here defined as the time between rising and recession limbs of a discharge peak (Fd), but also as the cumulative time when multiple discharge peaks occurred (Fd_c); mean discharge (Q_m); maximum discharge (Q_{max}); the time of rise to reach a peak discharge (Tr); water yield, expressed as the total depth of water during a discharge peak (Wt), but also the cumulative depth of water registered during multiple peaks (Wt_c); flood intensity, here defined as the discharge speed to reach the peak [$F_i = (Q_{max}–Q_b)/Tr$]; and a dummy variable to represent seasonality (S).

Water quality variables included SS, POC, and DOC mean and maximum concentration values monitored during a discharge peak (SSC_m, SSC_{max}, POC_m, POC_{max}, DOC_m, and DOC_{max}); SS, POC, and DOC loads to the reservoir during a discharge peak (SS_t, POC_t, and DOC_t); and the cumulative loads when multiple peaks occurred (SS_{ct}, POC_{ct}, and DOC_{ct}) (Table 2).

A Pearson correlation matrix that included all the above-mentioned variables was generated for all 35 peak discharges registered in Enxoé during the 21 flood events monitored. DOC information was only generated for 23 peak discharges since the monitoring of some discharge peaks was missed as data were limited to the number of samples taken manually and with the automatic sampler as referred above.

Identification of POC and DOC sources

For each flood event, the analysis the C–Q relationships for POC and DOC was performed with the approach proposed by Butturini et al. (2006). The shape, rotational patterns and trends of hysteretic loops of each determinand are here described with two parameters: the changes in solute concentrations (ΔC), and the overall dynamics of each hysteretic loop (ΔR). ΔC (%) describes the relative changes in solute concentration and hysteresis trend, as follows:

$$\Delta C = (C_s - C_b)/C_{max} \times 100 \quad (3)$$

where C_b and C_s are the solute concentrations at base flow and during peak flow, respectively, and C_{max} is the highest concentration observed in the stream during a storm. The ΔR (%) descriptor integrates information about the magnitude (area) and direction (rotational pattern) of the C–Q hysteresis, as follows:

$$\Delta R = R \times A_h \times 100 \quad (4)$$

where A_h is the area of the C–Q hysteresis, estimated after standardizing discharges and concentrations to a unity scale, and R summarizes the rotational pattern of the C–Q hysteresis.

The variability of POC and DOC hysteresis descriptors is described in the unity plane ΔC vs. ΔR, where four regions can be identified, according to flushing/dilution of the constituent and the hysteresis loop sense (clockwise or anticlockwise). All this information allows clarifying the source of POC and DOC, and separating different types of floods.

Table 1 Storm event parameters including antecedent variables, characterizing the situation prior to peak flow, and storm event variables (precipitation and discharge)

No.	P1 (mm)	P5	P10	Pe	Fd (h)	Fd_c	Tr	F_i (m^3 min^{-2})	Wt (hm^3)	Wt_c	Q_m (m^3 s^{-1})	Q_{max}	Q_b	Q_a
1	31.4	31.5	40.6	37.1	51.6	51.6	1.0	3.51	0.045	0.045	1.34	3.59	0.08	0.08
2	16.6	16.6	16.7	60.1	27.6	27.6	0.5	8.24	0.157	0.157	2.51	5.18	1.06	1.06
2	5.6	60.3	60.4	60.1	8.3	35.9	6.8	1.37	0.132	0.290	6.90	10.46	1.13	5.18
2	5.6	60.3	60.4	60.1	11.8	47.7	2.8	0.71	0.215	0.505	6.08	8.20	6.20	10.46
3	10.6	38.7	39.6	84.1	47.4	47.4	9.0	3.10	1.355	1.355	7.81	27.98	0.04	0.04
3	18.2	69.4	70.3	84.1	38.2	85.6	19.1	0.40	0.575	1.930	4.21	8.26	0.68	27.98
3	14.7	84.1	84.5	84.1	41.5	127.1	13.1	0.45	0.623	2.553	4.14	8.93	2.97	8.26
4	18.8	18.9	55.9	21.7	92.3	92.3	25.2	0.16	0.497	0.497	1.48	4.20	0.12	0.12
5	6.4	13.1	34.8	13.0	70.3	70.3	4.0	0.67	0.265	0.265	1.04	3.54	0.87	0.87
6	6.4	13.5	25.5	6.6	63.1	63.1	4.0	1.36	0.333	0.333	1.51	5.51	0.07	0.07
7	18.5	23.5	23.6	32.7	5.8	5.8	3.5	1.65	0.081	0.081	3.82	7.17	1.40	1.40
7	18.5	23.5	23.6	32.7	23.4	29.2	3.5	1.08	448.1	0.529	5.32	9.46	5.68	7.17
7	13.2	36.6	36.8	32.7	40.1	69.3	4.3	2.58	0.782	1.310	5.32	13.76	2.80	9.46
8	27.8	52.7	93.6	27.9	13.4	13.4	6.8	0.76	0.253	0.253	5.21	10.64	0.39	0.39
8	27.8	52.7	93.6	27.9	29.2	42.6	5.3	0.55	0.692	0.944	6.56	19.74	3.80	10.64
9	45.6	45.8	45.8	77.0	40.3	40.3	8.5	0.70	0.162	0.162	0.94	6.20	0.24	0.24
10	36.5	66.9	66.9	68.2	29.4	29.4	2.0	1.17	0.069	0.069	0.64	2.35	0.01	0.01
11	14.4	37.3	76.1	37.3	35.5	35.5	4.0	0.58	0.153	0.153	0.08	2.35	0.05	0.05
12	26.9	27.8	45.9	26.9	1.8	1.8	0.5	5.82	0.010	0.010	1.39	3.01	0.10	0.10
13	8.4	33.4	42.8	19.7	4.3	4.3	2.0	2.13	0.048	0.048	3.04	4.26	0.01	0.01
14	24.2	43.3	76.7	33.8	28.0	28.0	4.5	2.83	0.335	0.335	3.29	12.77	0.02	0.02
14	9.5	41.5	75.0	33.8	13.3	41.3	8.8	0.55	0.099	0.433	2.17	4.87	0.01	12.77
15	40.3	49.2	90.8	49.4	12.8	12.8	2.3	1.35	0.059	0.059	1.25	3.13	0.10	0.10
15	40.3	49.2	90.8	49.4	19.8	32.5	8.0	0.33	0.083	0.142	1.17	2.69	0.02	3.13
16	14.7	17.4	29.1	14.8	46.8	46.8	10.3	0.41	0.227	0.227	1.34	4.18	0.01	0.01
16	3.5	20.7	21.2	14.8	10.0	56.8	0.3	7.63	0.035	0.262	0.97	2.46	0.02	0.02
17	15.7	17.4	20.5	21.0	20.5	20.5	2.8	1.35	0.109	0.109	1.46	3.72	0.02	0.02
18	7.1	19.6	21.4	85.4	53.2	53.2	9.0	0.70	0.458	0.458	1.77	6.37	0.05	0.05
18	22.0	43.9	45.7	85.4	31.5	84.7	6.0	0.98	0.382	0.840	3.38	5.94	0.09	6.37
18	11.9	55.0	57.6	85.4	84.0	168.7	3.1	4.94	0.156	0.996	3.55	17.60	2.39	5.94
18	16.4	42.3	86.2	85.4	64.8	233.5	8.8	0.59	0.425	1.421	1.82	5.34	0.18	17.60
19	21.1	23.8	53.2	21.0	29.3	29.3	5.8	1.42	0.347	0.347	3.28	8.29	0.10	0.10
20	9.8	42.9	45.6	12.8	43.0	43.0	2.5	1.68	0.425	0.425	2.73	4.26	0.07	0.07
21	32.3	36.7	66.2	45.8	68.0	68.0	11.3	1.45	0.891	0.891	3.63	16.40	0.09	0.09
21	5.9	43.1	52.3	45.8	32.3	100.3	3.3	1.36	0.285	1.176	2.45	4.60	0.18	16.40

Results

Hydro-climatological context

Twenty-one flood events were registered between September, 2010 and August, 2013 (Fig. 2). These events took place during autumn (10), winter (8), and spring (3). Table 1 summarizes the main characteristics of all flood events monitored. The Enxoé River normally exhibited no flow or ephemeral conditions from June to October. In the beginning of each hydrological year (September/October), the first rain events generated flow peaks that were quickly reduced as the soil was not fully saturated and groundwater flow was greatly diminished. From October to December, the soil became increasingly saturated with successive heavy rains. Subsurface flow was enhanced during this period, resulting most times in flood events with multiple discharge peaks. From December to April, the response to rain events still existed as the soil continued to be saturated. Groundwater flows were maintained for longer periods, but still tended to fall quickly, especially during months with less rain (January/February). Hence, flow in

Table 2 Concentrations and transport rates of suspended sediments (SS), particulate organic carbon (POC), and dissolved organic carbon (DOC) during the 21 flood events monitored

No.	SSC_m (mg L^{-1})	SSC_{max}	SS_t (t)	SS_{ct}	POC_m (mg L^{-1})	POC_{max}	POC_t (t)	POC_{ct}	DOC_m (mg L^{-1})	DOC_{max}	DOC_t (t)	DOC_{ct}
1	217.0	708.0	25.5	25.5	9.72	31.72	1.14	1.14	9.50	10.50	0.30	0.30
2	319.3	1027.1	61.8	61.8	14.30	46.02	2.77	2.77	7.63	9.77	0.47	0.47
2	475.7	696.3	58.7	120.4	21.31	31.19	2.63	5.40	7.23	18.38	2.47	2.94
2	260.8	529.3	84.8	205.2	11.69	23.71	3.80	9.19	6.89	9.42	2.96	5.90
3	119.5	494.6	174.0	174.0	5.37	20.92	7.79	7.79	–	–	–	–
3	126.1	298.5	94.2	268.2	5.61	13.11	4.22	12.02	–	–	–	–
3	122.3	334.1	98.7	366.8	5.51	14.75	4.42	16.43	–	–	–	–
4	30.8	113.0	29.4	29.4	1.38	5.02	1.32	1.32	–	–	–	–
5	18.2	88.1	9.9	9.9	0.81	3.91	0.45	0.45	–	–	–	–
6	27.8	630.8	13.4	13.4	1.25	28.26	0.60	0.60	–	–	–	–
7	117.8	275.0	18.8	18.8	5.28	12.32	0.84	0.84	5.72	6.89	0.36	0.36
7	163.9	471.4	86.1	104.9	7.34	21.12	3.86	4.70	12.18	14.08	4.78	5.14
7	224.6	757.6	212.7	317.5	10.06	33.94	9.53	14.23	14.58	11.32	3.60	8.74
8	157.3	815.5	46.2	46.2	5.97	13.11	2.07	2.07	14.10	15.14	1.11	1.11
8	133.2	292.7	209.7	255.9	7.05	36.53	9.40	11.46	14.68	15.67	5.00	6.11
9	422.9	863.6	72.2	72.2	18.95	38.69	3.23	3.23	13.80	18.06	1.70	1.70
10	217.8	411.6	1.5	1.5	9.58	18.44	0.05	0.05	0.59	1.25	0.03	0.03
11	7.7	10.2	1.8	1.8	0.35	0.46	0.07	0.07	5.24	6.11	0.77	0.77
12	743.3	3790.1	5.7	5.7	33.30	169.80	0.25	0.25	13.79	15.50	0.34	0.34
13	720.7	1153.0	33.8	33.8	32.29	51.66	1.52	1.52	14.22	16.18	1.22	1.22
14	548.5	3519.4	378.3	378.3	24.58	157.67	16.95	16.95	–	–	–	–
14	523.2	1410.0	80.4	458.7	23.44	63.17	3.60	20.55	11.79	18.99	1.23	1.23
15	254.0	985.5	11.8	11.8	11.38	44.15	0.53	0.53	10.46	19.11	1.07	1.07
15	129.7	401.4	15.7	27.5	5.81	17.98	0.70	1.23	7.51	8.20	0.93	2.00
16	111.8	212.7	31.5	31.5	5.01	9.53	1.41	1.41	6.89	11.51	1.43	1.43
16	99.9	114.7	3.7	35.2	4.47	5.14	0.17	1.58	7.11	8.77	1.55	2.98
17	251.6	1431.2	41.1	41.1	11.27	64.12	1.84	1.84	3.50	5.29	1.37	1.37
18	126.6	718.0	50.1	50.1	5.67	32.17	2.24	2.24	5.91	9.55	0.97	0.97
18	129.6	457.7	60.6	110.7	5.81	20.51	2.72	4.96	–	–	–	–
18	113.6	1065.3	401.6	512.3	5.09	47.72	17.99	22.95	7.03	10.01	1.62	2.59
18	43.0	212.4	31.1	543.4	1.93	9.52	1.39	24.34	–	–	–	–
19	124.7	577.9	61.6	61.6	5.58	25.89	2.76	2.76	8.54	10.01	0.34	0.34
20	78.2	387.4	39.3	39.3	3.50	17.36	1.76	1.76	–	–	–	–
21	106.5	622.0	158.1	158.1	4.77	27.87	7.08	7.08	–	–	–	–
21	56.4	205.7	20.8	178.9	2.53	9.21	0.93	8.02	–	–	–	–

the Enxoé River was mostly influenced by rainfall events, whereas the effect of groundwater table was not significant.

Total precipitation amounted 695, 270, and 570 mm during the 2010/2011, 2011/2012, and 2012/2013 hydrological years (i.e., from September to August of the following year), respectively. The first hydrological year can thus be classified as humid, the second as very dry, and the third as within average ($\approx$500 mm). River discharge reflected those rainfall amounts, with annual water yield reaching 28.73, 1.27, and 10.14 hm^3 in the corresponding hydrological years.

POC and DOC concentrations and relationships with hydro-climatological variables

Figure 3 present POC and DOC concentrations monitored between September, 2010 and August, 2013. POC concentrations ranged from 0.49 to 88.93 mg L^{-1}, with the highest value being detected in October, 2010 (event 2). POC averaged 9.52 mg L^{-1} during the entire monitored period (standard deviation, $\sigma = 13.32$ mg L^{-1}). On the other hand, DOC concentrations ranged from 0.25 to 25.75 mg L^{-1}, with the highest value being monitored in

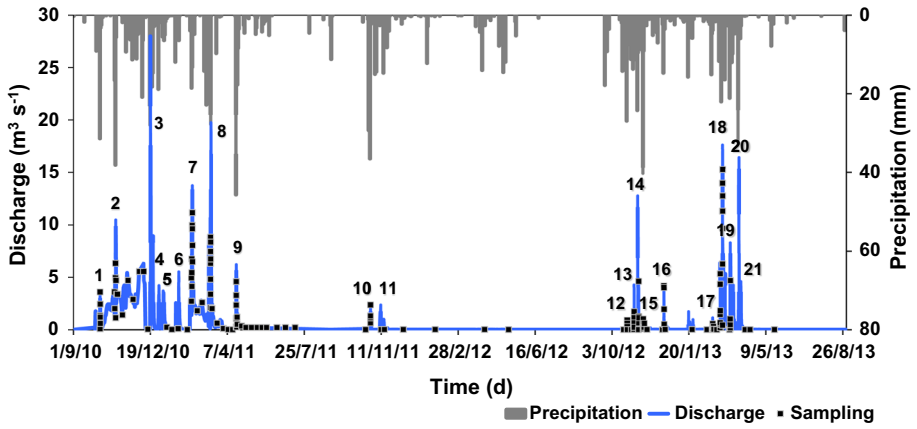

Fig. 2 Precipitation (mm) and discharge (m^3 s^{-1}) at the river Enxoé outlet between September, 2010 and August, 2013

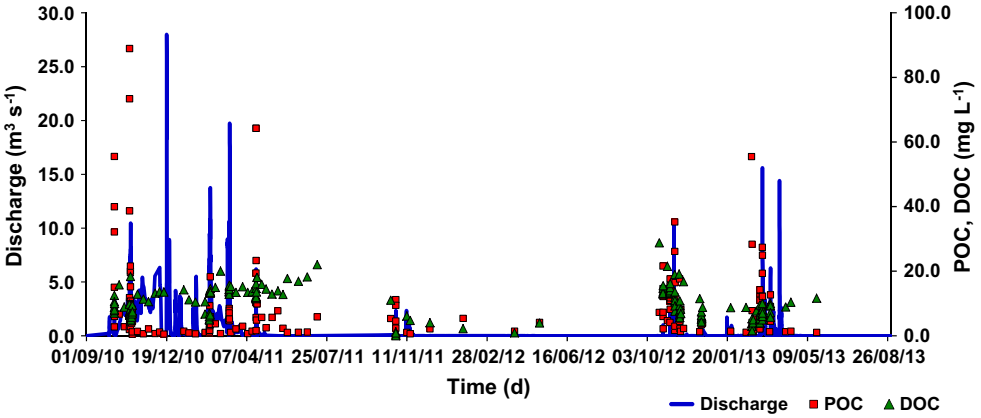

Fig. 3 Discharge, particulate organic carbon (POC), and dissolved organic carbon (DOC)

October, 2012 (event 12). DOC averaged 10.27 mg L^{-1}, but σ was only 4.69 mg L^{-1}. Thus, flood events had greater effect in POC than in DOC variability.

Figure 4 present the relationships between POC and SSC and turbidity values documented in Ramos et al. (2014). These relationships show a R^2 higher than 0.90, confirming POC adsorption onto SS. Hence, POC yields were estimated based on these close relationships to reduce uncertainty.

POC and DOC loads

Figure 5 present POC and DOC loads to the Enxoé reservoir between September, 2010 and August, 2013. POC loads totalized 173.7 t (3.86 t km^{-2}), but the amounts exported varied considerably throughout the years. In 2010/2011, POC losses reached 2.15 t km^{-2}. The second year only registered exports of 0.06 t km^{-2} due to an extended drought. Finally, POC yields reached 1.66 t km^{-2} during 2012/2013.

Flood events contributed with 57.2 and 85.7 % of POC exports during the first and third years, respectively. During 2011/2012, the events registered did not produce significant water yield, and thus POC losses were more distributed along the year. The same behavior had already been found for SS (Ramos et al. 2014). The most significant POC exports were registered in autumn and spring. During 2010/2011, events 2, 7, and 8 contributed with 9.5, 14.7, and 11.9 %, respectively, of the annual export. During 2012/2013, events 14 and 18 registered more than 60 % of the annual losses.

DOC loads to the Enxoé reservoir were slightly lower than POC exports (Fig. 5). DOC losses totalized 98.1 t (2.18 t km^{-2}). Again, the three hydrological years showed great variability, with DOC exports reaching 1.47, 0.03, and 0.68 t km^{-2} in 2010/2011, 2011/2012, and 2012/2013, respectively. Table 2 show few gaps in the DOC dataset which were inevitable since DOC data were limited to the number of samples taken manually and with the automatic sampler. Figure 6 show the relationship used to derive DOC losses when no measured data were available. This relationship was based on the high correlation found between DOC_{ct} and Wt_c in Table 3. Thus, having in mind that this approach may have led to significant uncertainty in some of the estimates (e.g., event 3), it seems as one of the best possible ways to provide an estimate of DOC exports for the entire monitored period (Fig. 5).

Flood events contributed with 64.5, 63.0, and 95.2 % of DOC exports during 2010/2011, 2011/2012, and 2012/2013, respectively. The most significant DOC exports were also registered in autumn and spring. Events 3 and 7 registered 20.4 and 13.2 %, respectively, of the DOC lost during 2010/2011. Event 11 seems to have been the main responsible for DOC losses during 2011/2012. Finally, events 14, 18, 20, and 21 contributed with 68.2 % of the annual losses during the last year.

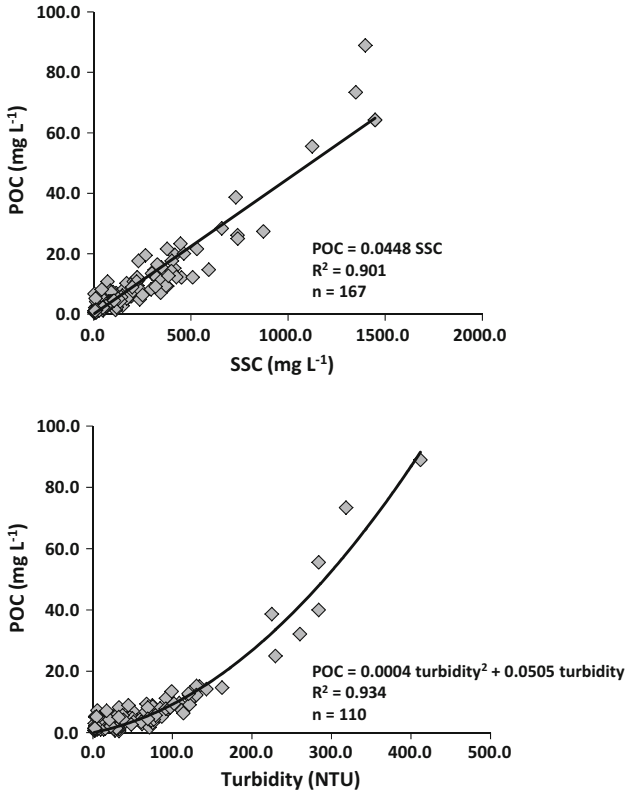

Fig. 4 Relationship between suspended sediment concentration (SSC) and particulate organic carbon (POC) (*top*), and between turbidity and POC (*bottom*)

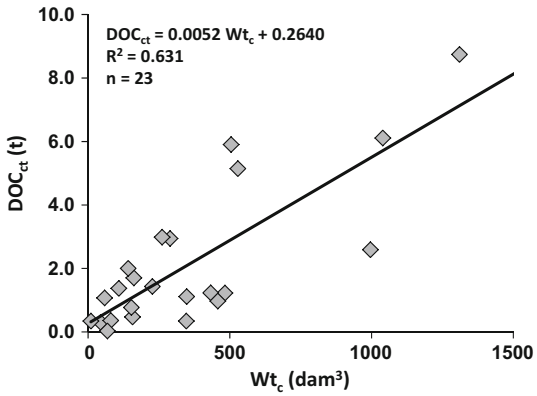

Fig. 6 Relationship between water yield during flood events (Wt_c) and total dissolved organic carbon exports during flood events (DOC_{ct})

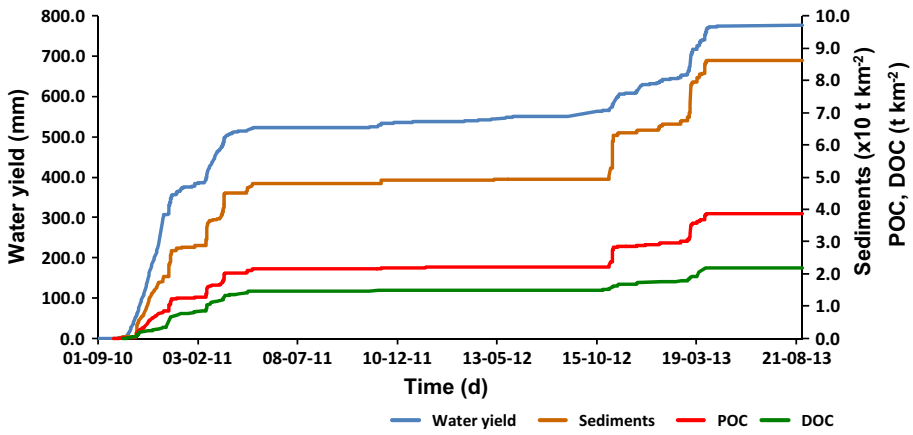

Fig. 5 Cumulative water yield, suspended sediments (in Ramos et al. 2014), particulate organic carbon (POC), and dissolved organic carbon (DOC) transport in the Enxoé catchment between September, 2010 and August, 2013

Hysteresis patterns

POC-discharge and DOC-discharge relationships were analyzed for most of the events monitored in the Enxoé catchment. Those that did not produce sufficient detailed information as a result of data limitation were not analyzed for their hysteresis patterns.

Figure 7 show the unity plane ΔC vs. ΔR of Butturini et al. (2006), and summarizes POC-Q and DOC-Q hysteresis relations during the monitored period. POC components were located in regions A and D, indicating a flushing behavior (positive ΔC). Most flood events registered during autumn were located in region A, presenting a clockwise hysteresis loop trajectory (positive ΔR). Events 15 and 16 were the exception, registering anticlockwise loop trajectories in all discharge peaks (region D). Winter flood events registered mixed (figure-of-eight-shaped hysteresis loops; $\Delta R = 0$) or anticlockwise loop trajectories (negative ΔR) with small magnitudes ($-20\ \% < \Delta R < 0\ \%$). Spring flood events showed contrasting behaviors, with the event monitored during 2010/2011 registering an anticlockwise

Table 3 Pearson correlation matrix between POC and DOC concentrations and loads, and hydro-climatological variables

	S	P1	P5	P10	Pe	Fd	Fd_c	Tr	F_i	Wt	Wt_c	Q_m	Q_{max}	Q_b
POC_m	*−0.410*	0.130	0.080	0.011	−0.062	**−0.562**	**−0.444**	−0.268	0.264	*−0.350*	−0.324	0.054	−0.070	−0.055
POC_{max}	−0.277	0.184	−0.055	0.026	−0.110	−0.302	−0.300	−0.278	*0.368*	−0.196	−0.237	−0.041	0.058	−0.102
POCt	0.081	−0.008	0.271	0.188	0.248	0.257	0.248	0.040	0.218	*0.394*	*0.358*	**0.469**	***0.737***	0.305
POC_{ct}	0.105	−0.186	**0.456**	*0.403*	**0.441**	0.226	***0.675***	0.206	−0.021	0.311	***0.662***	*0.350*	**0.452**	0.292
DOC_m	0.271	0.169	0.033	0.214	−0.280	−0.171	−0.131	0.097	0.089	0.368	0.301	0.362	0.370	0.191
DOC_{max}	0.081	0.083	0.163	0.284	−0.066	−0.243	−0.135	0.276	−0.054	0.082	0.091	0.323	0.240	0.054
DOC_t	0.310	−0.192	0.185	0.066	−0.079	0.024	0.205	0.121	−0.109	***0.707***	***0.693***	***0.701***	***0.670***	***0.792***
DOC_{ct}	0.225	−0.256	0.225	0.036	−0.047	0.059	0.319	0.025	−0.022	***0.728***	***0.809***	***0.662***	***0.631***	***0.768***

	Q_a	P_n	SSC_m	SSC_{max}	SS_t	SS_{ct}	POC_m	POC_{max}	POC_t	POC_{ct}	DOC_m	DOC_{max}	DOC_t	DOC_{ct}
POC_m	−0.113	−0.143	***1.000***	***0.770***	0.114	0.041	1.000							
POC_{max}	−0.172	−0.178	***0.770***	***0.988***	*0.369*	0.146	***0.773***	1.000						
POCt	0.143	0.288	0.112	*0.344*	***1.000***	***0.668***	0.119	*0.375*	1.000					
POC_{ct}	***0.639***	***0.756***	0.041	0.129	***0.668***	***1.000***	0.047	0.154	***0.668***	1.000				
DOC_m	0.313	0.134	*0.436*	0.339	0.229	0.243	*0.439*	0.343	0.229	0.243	1.000			
DOC_{max}	0.292	0.063	**0.554**	0.334	0.112	0.251	**0.556**	0.337	0.113	0.251	***0.782***	1.000		
DOC_t	***0.705***	**0.628**	−0.106	−0.228	*0.487*	*0.433*	−0.089	−0.138	*0.487*	*0.433*	*0.431*	0.327	1.000	
DOC_{ct}	***0.732***	***0.804***	−0.138	−0.219	**0.534**	**0.500**	−0.125	−0.149	**0.534**	*0.500*	0.370	0.154	***0.890***	1.000

Correlation is significant at $P < 0.001$ for underlined italic bold numbers, at $P < 0.01$ level for italic bold numbers, and $P < 0.05$ for italic numbers

trajectory, and the events monitored in 2012/2013 presenting clockwise trajectories.

Generally, the first discharge peaks of autumn floods showed larger dispersion of the *C–Q* hysteresis loops when compared with the remaining events. Those peaks presented a large area ($\Delta R > 20$ %) while all other events registered smaller magnitudes ($-20\ \% < \Delta R < 20\ \%$). Also, a significant number of events (especially those that occurred during winter) presented a ΔC close to 100 %, indicating that the concentration and the discharge peaks observed during the hysteresis loops were relatively close, i.e., the delay between concentration and discharge peaks was small.

DOC was mostly located in regions B and C of the unity plane ΔC vs. ΔR. DOC presented, in general, a dilution behavior (negative ΔC) during the entire monitored period. The only exceptions were observed during events 7 and 14, where some of the peak flows revealed a flushing behavior for DOC. The *C–Q* hysteresis loops observed during event 7, although revealing contrasting loop trajectories in the multiple discharge peaks monitored, presented always large magnitudes ($-20\ \% < \Delta R < 20\ \%$). Autumn and spring events presented, in general, an anticlockwise trajectory (negative ΔR). DOC transport during winter events was more erratic and no typical trajectories were identified.

Discussion

The large seasonal and annual variability observed in POC exports was mostly associated with variations in SS transport. POC and SS dynamics showed a strong correlation ($R^2 > 0.90$) (Fig. 4), which means that POC monitored at the outlet was mainly adsorbed onto SS. Ramos et al. (2014) showed that SS transport in Enxoé was related to variations in the stream transport capacity and particle availability. Sediments were stored at low flow and transported under high discharge conditions. Tillage operations carried out during autumn and spring in agricultural fields with annual crops, and pasturing the river bed during spring and summer were the main activities associated with soil erosion and particle availability. The high precipitation rates also registered especially during autumn when soil cover provided by crop residues had been removed and surface runoff were the main processes associated with the transfer of soil particles to the Enxoé reservoir. Thus, like SS loads, the most significant POC exports were registered in autumn and spring. These processes explain the significant correlations found between POC_m and S, Fd and Fd_c, and Wt; between POC_{max} and F_i; and also between POC loads (POC_t and POC_{ct}) and Fd_c, Wt_c, Q_{max}, Q_m, and rainfall (P5, P10, and Pe). Autumn and spring flood events registered, in general, higher magnitudes, leading to greater POC exports from the catchment, consistent with the

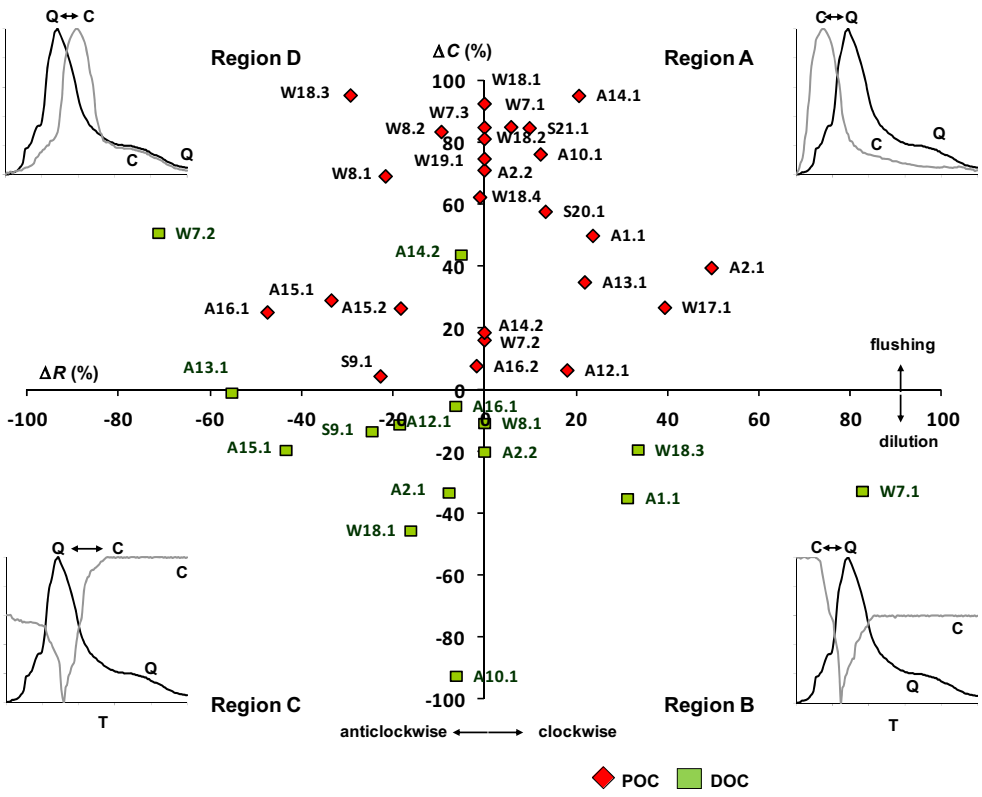

Fig. 7 Unity plane ΔC vs. ΔR for the *C–Q* hysteresis loops of particulate organic carbon (POC) and dissolved organic carbon (DOC). The marks *i,j* correspond to the *i*th flood event monitored (1–21) and the *j*th discharge peak (1–4) monitored during autumn (A), winter (W), and spring (S). Illustrations of typical *C–Q* relations are presented for each region of the unity plane

behaviors reported for different catchments in the Mediterranean region (e.g. Butturini et al. 2008; Oeurng et al. 2011; Cerro et al. 2013).

POC transported to the Enxoé River seems to have had mainly a terrestrial origin. During autumn, POC was transported along with sediments from deposits accumulated in the river bed due to pasturing, bank degradation, and temporary deposition, but also from arable lands located upstream and where tillage operations were carried out. The former, i.e., loads arriving from nearby locations explains the dominant loop trajectories and the flushing effect registered during the first peak discharge of autumn floods. The latter, i.e., sediments and POC arriving simultaneous from multiple locations explains the mixed trajectories registered in the following peak discharges of the flood events, when multiple peaks occurred. Table 4 summarize POC dynamics in the Enxoé catchment.

During autumn, POC loads had also an aquatic origin though. In Enxoé, the dominant loop trajectories and the flushing effect registered during the first peak flow of autumn floods can also be partially explained by the transfer of POC accumulated in pools formed in the river bed during summer, which were enriched with the accumulation of nutrients and organic matter. However, the contribution of this component seems to be minor when comparing with POC exports from soil erosion monitored in Enxoé or with some reports available in literature from other catchments (e.g. Hélie and Hillaire-Marcel 2006). These authors reported that in the St. Lawrence River (Canada), aquatically produced POC dominates terrestrially derived organic matter (OM) throughout the system all year round, which does not happened in Enxoé. POC production in Enxoé seems to be more consistent with Lu et al. (2012), who refer that POC was mainly terrestrially produced in high turbid rivers (in our case, flash floods), whereas the contribution of aquatic biomass to POC increased evidently in low turbid rivers (in our case, pools formed during non-flood events). Those authors found that, in the Longchuanjiang catchment (Upper Yangtze basin, China), terrestrial production contributed 78 % to POC, and the rest of POC was due to aquatic origin.

During winter, as sediment loads remained generally low, so did POC exports. This was attributed to the depletion of the sediment deposits in the river bed (Asselman 1999). Hence, POC exports resulted from soil erosion in agricultural fields, as observed in the flushing anticlockwise or mixed patterns registered in the *C–Q* relation. During spring, POC presented also a terrestrial origin. Loads increased again as a result of high precipitation values and soil erosion. Tillage operations were carried out throughout the catchment, and the cattle returned to pasturing near the river bed. These practices again promoted particle availability to runoff, i.e., flushing.

Table 4 Conceptual model of the source and transport of particulate organic carbon (POC) and dissolved organic carbon (DOC) in the river Enxoé catchment area

Season	POC	DOC
Autumn		
Source	Terrestrial/Aquatical (River banks)	Terrestrial (Agricultural fields)
Transfer	Runoff	Subsurface flow
Hysteresis pattern	Clockwise/Flushing	Anticlockwise/ Dilution
Winter		
Source	Terrestrial (Agricultural fields)	Terrestrial (Agricultural fields)
Transfer	Runoff	Subsurface flow
Hysteresis pattern	Mixed/Flushing	Mixed/Dilution
Spring		
Source	Terrestrial (River banks/ Agricultural fields)	Terrestrial (Agricultural fields)
Transfer	Runoff	Subsurface flow
Hysteresis pattern	Mixed/Flushing	Anticlockwise/ Dilution
Summer		
Transfer	No flow	No flow

Clockwise and anticlockwise trajectory loops were thus observed during spring whenever POC was transported predominantly from river deposits (or temporary pools) or from more distant locations upstream, respectively.

The close relationship found between SS and POC is easy to understand if we acknowledge that POC represents all physically present organic particles (e.g. leaves), as opposed to DOC, which represents the colloidal and truly dissolved organic matter dominated by humic and fulvic acids (Worrall et al. 2005). Nonetheless, the linear relation found between SS and POC (Fig. 4) is different than the relationships reported by Oeurng et al. (2011) and Cerro et al. (2013). These authors showed that POC–SSC relationship may be hyperbolic due to changes in organic matter sources. High POC % may correspond to phytoplankton production during low-flow periods, and lower content of POC during high flow periods may result from soil erosion or from resuspended inorganic sediments from the main channel. Although pools formed in the Enxoé temporary river during non-flood events were largely enriched with organic matter, the hyperbolic relationship between POC and SSC was not found here since the temporary pools also contained a large portion of sediments as a result of bank degradation and pasturing. Thus, in the Enxoé River high SS exports will likely always coincide with high POC loads if agricultural practices carried out in the catchment are not modified.

DOC dynamics also presented a strong seasonal and annual variability, but flood events had less effect in DOC than in POC variability. Storm pulses of POC are often reported in literature as transients (Jung et al. 2012; Lu et al. 2012; Lloret et al. 2013). This seems to be the case in Enxoé, where POC/TOC (total OC) increased from 0.19 (average value) during non-flood events to 0.47 during flood events. In contrast, DOC/TOC decreased from 0.81 to 0.53. Thus, while POC exports increased with discharge, DOC loads were smaller due to dilution, with concentrations only increasing when discharge was reduced. Although DOC is reported in literature as the main component in riverine organic C in large rivers (Moreira-Turcq et al. 2003; Hélie and Hillaire-Marcel 2006; Worrall et al. 2012), unusually high concentrations and export POC exceeding those of DOC have been observed in streams draining upland forested watersheds and small mountainous rivers during storm events (Jung et al. 2012), a behavior more consistent with the Enxoé catchment.

During the monitored period, DOC concentrations monitored at the Enxoé outlet were more constant than POC concentrations, and thus correlations between DOC_m, DOC_{max} and the hydro-climatological variables were weaker or non-significant. Nonetheless, DOC yield (DOC_t and DOC_{ct}) was correlated to water yield (Wt and Wt_c), to the number of peak flows (P_n) observed during flood events, and to their transport capacity (Q_m and Q_{max}). Thus, these variables seem to have been the main factors controlling DOC exports from the Enxoé catchment during the monitored period.

DOC losses were again monitored mostly during autumn and spring. DOC showed, in general, a dilution behavior throughout the entire monitored period, with concentrations monitored at the outlet usually decreasing with the arrival of the discharge peak, and increasing again in the recession limbs of flood events. Thus, DOC concentration in surface runoff was lower than in subsurface flow. Consequently, hysteresis patterns observed during the monitored events showed predominantly anticlockwise trajectories, indicating that DOC was mostly transported from more distant regions, such as arable lands, olive groves, etc. (Table 4). Events 1 and 7 were the exceptions (Fig. 7). These events presented clockwise hysteresis loops during the first discharge peaks, indicating a possible transport of DOC produced in the enriched temporary pools formed in the river bed during non-flood events. Oeurng et al. (2011) and Strohmeier et al. (2013) found similar dilution patterns in catchments in France and Germany, respectively, but the latter only observed clockwised hysteresis patterns in the *C–Q* relationship. On the other hand, Butturini et al. (2008), Cerro et al. (2013) observed a dominant DOC flushing behavior in Spanish catchments. However, Butturini et al. (2006) could not find a consistent and recurrent pattern explaining DOC transport in three Mediterranean streams during storms.

In Enxoé, DOC appears to be also dominated by terrestrially derived OM with some influence of DOC derived from aquatically produced POC in summer, which is in agreement with many reports found in literature (Raymond and Bauer 2001; Hélie and Hillaire-Marcel 2006; Worrall et al. 2012; Oh et al. 2013). DOC resulted mainly from soil weathering processes, the mineralization of crop residues and other organic wastes, and the mineralization of the soil humus fraction. The main transfer mechanism to the river was subsurface flow. DOC transport was thus dependent of the soil physical and hydraulic characteristics, i.e., soil texture, soil porosity, and soil hydraulic properties, which influenced the delay in the *C–Q* relationship. Subsurface flow is thus the same mechanism that was also associated NO_3^- exports in Enxoé (Ramos et al. 2014). However, the origin and flow-paths of DOC and NO_3^- seem fundamentally different, since NO_3^- showed a flushing behavior during autumn due to fertilization practices.

The Enxoé catchment registered average POC and DOC yields of 1.29 and 0.73 t km^{-2} $year^{-1}$, respectively. POC average yields were thus higher than those obtained by Veyssy et al. (1999) for the Garonne catchment in southern France (0.80 t km^{-2}). They were also higher than those observed by Cerro et al. (2013) for the Alegria catchment, in northern Spain (0.54 t km^{-2}), but lower than the values monitored by Oeurng et al. (2011) in the Save catchment (1.80 t km^{-2}), also in southern France. On the other hand, DOC average yields were similar to those found by Veyssy et al. (1999), Oeurng et al. (2011), Cerro et al. (2013), Strohmeier et al. (2013), which ranged between 0.70 and 0.85 t km^{-2} $year^{-1}$. However, the Enxoé catchment registered an extensive drought during the hydrological year of 2011/2012 which lowered average annual yields significantly. Results show that POC and DOC losses reached up to 2.15 and 1.47 t km^{-2}, respectively, during the first hydrological year. These values are thus comparable higher than the values monitored in Spain and France. The high precipitation rates and soil erosion may explain the values registered in Enxoé, since agriculture and pasturing were not very intensive. The values registered in Enxoé are also incomparably lower than those found by Alexander et al. (1996), Hope et al. (1997), Moreira-Turcq et al. (2003), Worrall et al. (2012), Lloret et al. (2013) in organic soils or tropical regions.

Conclusion

This study shows that POC and DOC dynamics in the Enxoé temporary river during storms were different than those acknowledged for major rivers located in the

Mediterranean region. POC registered a flushing behavior during flood events, especially during autumn and spring, similarly to suspended sediments dynamics. Clockwised trajectory loops in the *C–Q* relationship were predominantly observed in autumn. During this period, POC loads resulted mostly from sediments deposited in the river bed due to bank degradation and pasturing. Aquatically produced POC was only a minor component of POC exports, and was flushed during the first discharge peaks of autumn events. During winter and spring, anticlockwise or mixed trajectory loops were mainly registered, indicating that POC exports continued having predominantly a terrestrial origin. Soil erosion in agricultural fields was here the main process contributing to POC exports during those periods. POC yields varied between 0.06 and 2.15 t km^{-2}, with exports being relatively high during humid years due to high precipitation rates and soil erosion.

The effect of flood events in DOC variability was smaller than that observed for POC. DOC registered a recurrent dilution behavior during the studied period. POC concentrations in subsurface runoff were thus higher than in surface runoff. Anticlockwise trajectory loops in the *C–Q* relationship were, in general, observed during flood events. DOC had mostly a terrestrial origin, resulting mainly from soil weathering processes, the mineralization of crop residues and other organic wastes, and the mineralization of the soil humus fraction. DOC yields ranged from 0.03 to 1.47 t km^{-2}, with exports being also depended on rainfall.

Acknowledgments This research was performed within the framework of the AGUAFLASH project (SOE1/P2/F146, EU Interreg SUDOE IVB program, http://www.aguaflash-sudoe.eu), and the EUTROPHOS project (PTDC/AGR-AAM/098100/2008, Fundação para a Ciência e a Tecnologia).

References

Alexander RB, Slack J, Ludtke AS, Fitzgerald KK, Schertz TL (1996) Data from selected US geological survey national stream water-quality monitoring networks. Water Resour Res 34:2401–2405

APHA (1998) Standard methods for the examination of water and wastewater. Prepared and published jointly by American Public Health Association, American Water Works Association and Water Environment Federation, Washington DC

Asselman NEM (1999) Suspended sediment dynamics in a large drainage basin: the River Rhine. Hydrol Process 13:1437–1450

Bowes MJ, House WA, Hodgkinson RA, Leach DV (2005) Phosphorus-discharge hysteresis during storm events along a river catchment: the River Swale, UK. Water Res 39:751–762

Butturini A, Gallart F, Latron J, Vazquez E, Sabater F (2006) Cross-site comparison of variability of DOC and nitrate C–Q hysteresis during the autumn–winter period in three Mediterranean headwater streams: a synthetic approach. Biogeochemistry 77:327–349

Butturini A, Alvarez M, Bernal S, Vazquez E, Sabater F (2008) Diversity and temporal sequences of forms of DOC and NO^{3-}discharge responses in an intermittent stream: predictable or random succession? J Geophys Res 113:G03016. doi:10.1029/2008JG000721

Cerro I, Sanchez-Perez JM, Ruiz-Romera E, Antigüedad I (2013) Variability of particulate (SS, POC) and dissolved (DOC, NO^3) matter during storm events in the Alegria agricultural watershed. Hydrol Process. doi:10.1002/hyp.9850

Evans C, Davies TD (1998) Causes of concentration/discharge relationship hysteresis and its potential as tool for analysis of episode hydrochemistry. Water Resour Res 34:129–137

Hall FR (1970) Dissolved solids-discharge relationships: 1. Mixing models. Water Resour Res 6:845–850. doi:10.1029/WR006i003p00845

Hélie JF, Hillaire-Marcel C (2006) Sources of particulate and dissolved organic carbon in the St. Lawrence River: isotopic approach. Hydrol Process 20:1945–1959

Hope D, Billett MF, Milne R, Brown TAW (1997) Exports of organic carbon in British rivers. Hydrol Process 11:325–344

House WA, Warwick MS (1998) Hysteresis of the solute concentration/discharge relationship in rivers during storms. Water Resour 32:2279–2290

Instituto da Água (2008) Poluição provocada por nitratos de origem agrícola. Relatório (2004–2007). Publicação conjunta do MAOTDR e MADRP, Lisboa, Portugal

Jung BJ, Lee HJ, Jeong JJ, Owen J, Kim B, Meusburger K, Alewell C, Gebauer G, Shope C, Park JH (2012) Storm pulses and varying sources of hydrologic carbon export from a mountainous watershed. J Hydrol 440–441:90–101

Lillebø AI, Morais M, Guilherme P, Fonseca R, Serafim A, Neves R (2007) Nutrient dynamics in Mediterranean temporary streams: a case study in Pardiela catchment (Degebe River, Portugal). Limnologica 37:337–348

Lloret E, Dessert C, Pastor L, Lajeunesse E, Crispi O, Gaillardet J, Benedetti MF (2013) Dynamic of particulate and dissolved organic carbon in small volcanic mountainous tropical watersheds. Chem Geol 351:229–244

Lu XX, Li S, He M, Zhou Y, Li L, Ziegler AD (2012) Organic carbon fluxes from the upper Yangtze basin: an example of the Longchuanjian River, China. Hydrol Process 26:1604–1616

Moreira-Turcq P, Seyler P, Guyot JL, Etcheber H (2003) Exportation of organic carbon from the Amazon River and its main tributaries. Hydrol Process 17:1329–1344

Némery J, Mano V, Coynel A, Etcheber H, Moatar F, Maybeck M, Belleudy P, Poirel A (2013) Carbon and suspended sediment transport in an impounded alpine river (Isère, France). Hydrol Process 27:2498–2508

Oeurng C, Sauvage S, Coynel A, Maneux E, Etcheber H, Sánchez-Pérez JM (2011) Fluvial transport of suspended sediment and organic carbon during flood events in a large agricultural catchment in southwest France. Hydrol Process 25:2365–2378

Oh NH, Pellerin BA, Bachand PAM, Hernes PJ, Bachand SM, Ohara N, Kavvas ML, Bergamaschi BA, Horwath WR (2013) The role of irrigation runoff and winter rainfall on dissolved organic carbon loads in an agricultural watershed. Agric Ecosyst Environ 179:1–10

Ramos TB, Gonçalves MC, Branco MA, Brito D, Rodrigues S, Sánchez-Pérez JM, Sauvage S, Prazeres A, Martins JC, Fernandes ML, Pires FP (2014) Sediment and nutriente dynamics during storm events in the Enxoé temporary river, Southern Portugal. Catena (under review)

Raymond PA, Bauer JE (2001) Riverine export of aged terrestrial organic matter to the North Atlantic Ocean. Nature 409:497–500

Strohmeier S, Knorr KH, Reichert M, Frei S, Fleckenstein JH, Peiffer S, Matzner E (2013) Concentrations and fluxes of dissolved organic carbon in runoff from a forested catchment: insights from high frequency measurements. Biogeosci Disc 10:905–916

Tzoraki O, Nikolaidis NP (2007) A generalized framework for modeling the hydrologic and biochemical response of a Mediterranean temporary river basin. J Hydrol 346:112–121

Veum KS, Goyne KW, Motavalli PP, Udawatta RP (2009) Runoff and dissolved organic carbon loss from a paired-watershed study of three adjacent agricultural watersheds. Agric Ecosyst Environ 130:115–122

Veyssy E, Etcheber H, Lin RG, Buat-Menard P, Maneux E (1999) Seasonal variation and origin of particulate organic carbon in the lower Garonne River at La Reole (Southwestern France). Hydrobiologia 391:113–126

Worrall F, Swank WT, Burt T (2005) Fluxes of inorganic carbon from two forested catchments in the Appalachian Mountains. Hydrol Process 19:3021–3035

Worrall F, Davies H, Bhogal A, Lilly A, Evans M, Turner K, Burt T, Barraclough D, Smith P, Merrington G (2012) The flux of DOC from the UK–Predicting the role of soils, land use and net watershed losses. J Hydrol 448–449:149–160

Zhu Q, Schmidt JP, Bryant RB (2012) Hot moments and hot spots of nutrient losses from a mixed land use watershed. J Hydrol 414–415:393–404